

AN ADAPTIVE FUNCTIONAL REGRESSION FRAMEWORK FOR SPATIALLY HETEROGENEOUS SIGNALS IN SPECTROSCOPY

Federico Ferraccioli¹, Alessandro Casa², and Marco Stefanucci³

¹*Department of Statistical Sciences, University of Padova, Italy*

²*Faculty of Economics and Management, Free University of Bozen-Bolzano, Italy*

³*Department of Economics and Finance, University of Rome Tor Vergata, Italy*

Abstract

The attention towards food products characteristics, such as nutritional properties and traceability, as well as towards the adherence of production systems to environmental and ethical procedures, has risen substantially in the recent years. Consequently, we are witnessing an increased demand for the development of modern tools to monitor, analyse and assess food quality, security, and authenticity. Within this framework, an essential set of data collection techniques is provided by vibrational spectroscopy. In fact, methods such as Fourier near-infrared (NIR) and mid-infrared (MIR) spectroscopy have been often exploited to analyze different foodstuffs. Nonetheless, existing statistical methods often struggle to deal with the challenges presented by spectral data, such as their high-dimensionality, paired with strong relationships among the wavelengths. Therefore, the definition of proper statistical procedures accounting for the intrinsic peculiarities of spectroscopy data is paramount.

In this work, motivated by two dairy science applications, we propose an adaptive functional regression framework for spectroscopy data. The method stems from the trend filtering literature, allowing the definition of a highly flexible and adaptive estimator able to handle different degrees of smoothness. We provide a fast optimization procedure that is suitable for both Gaussian and non-Gaussian scalar responses, and allows for the inclusion of scalar covariates. Moreover, we develop inferential procedures for both the functional and the scalar component thus enhancing not only the interpretability of the results, but also their usability in real world scenarios. The method is applied to two sets of MIR spectroscopy data, providing excellent results when predicting both milk chemical composition and cows' dietary treatments. Moreover, the developed inferential routine provides relevant insights, potentially paving the way for a richer interpretation and a better understanding of the impact of specific wavelengths on milk features.

Keywords: Adaptive Regression, Trend Filtering, Functional Data, Bootstrap, Spectroscopy

1 Introduction

In the past decades, increased consumers' attention towards food quality and security has fostered the development of new technologies to analyze different foodstuffs. More specifically, adherence to environmental-friendly procedures, product traceability, and quantification of the nutritional properties have become central topics on the agenda both of the public opinion and of the scientific community. Moreover, methods to assess food authenticity are increasingly important, as expensive products are often subject to fraud and adulteration.

In this framework, commonly adopted methodologies often require lengthy and expensive laboratory extraction routines to collect data, thus jeopardizing their usefulness. As a consequence, other alternatives have recently been proposed to overcome these drawbacks, with vibrational spectroscopy techniques currently playing a pivotal role. Methods such as Fourier

transform near-infrared (NIR) and mid-infrared (MIR) spectroscopy are known to be fast, relatively cheap, and nondisruptive ways to collect huge amounts of data on a plethora of materials. In fact, they have been used in different fields, ranging from medicine (Petrich, 2001; Talari et al., 2017) and astronomy (Keller et al., 2006; Tennyson, 2019), to food and animal science (Reid et al., 2006; Berzaghi and Riovanto, 2009; Porep et al., 2015).

In this work, we focus specifically on MIR spectroscopy, where the light is passed through a sample of a given material at a sequence of wavelengths in the mid-infrared region, activating the sample’s chemical bonds. This leads to an absorption of the energy from the light, the amount of which, evaluated at different wavelengths, creates the spectrum of the analyzed sample. Each spectrum contains an invaluable amount of information about the sample since, according to *Beer-Lambert Law* (Beer, 1852), the absorption of energy is specific to atoms and molecules and is proportional to the concentration of the corresponding chemical substance. As a consequence, nowadays spectral data are being used to predict different characteristics of a given material. With specific reference to the dairy framework, the one considered in this work, MIR spectroscopy showed promising results in predicting traits such as milk coagulation properties (Visentin et al., 2016), fatty acids (Soyeurt et al., 2006), protein and lactose concentration (De Marchi et al., 2014), energy efficiency and intake (McParland and Berry, 2016), as well as in discriminating between different cows’ dietary treatments (Frizzarin et al., 2021b).

Despite being widely used, the peculiar characteristics of spectroscopy data introduce statistical challenges that need to be addressed. First, spectral data lie in high-dimensional spaces, as each single spectrum usually consists of more than 1000 absorbance values measured at different wavelengths. Moreover, the relationships among variables are rather complex, often preventing the use of standard models developed for time-dependent data. In fact, even if adjacent spectral regions tend to be highly correlated, strong correlations are also observed among distant wavelengths, since the same chemical components can have several absorption peaks in distinct spectral regions. Lastly, as pointed out by Politsch et al. (2020), the underlying signal is often spatially heterogeneous. Therefore, flat spectral regions are often followed by more irregular ones, characterized by multiple peaks, posing cumbersome issues in the modelling process.

Both with regression and classification aims in mind, these data have been often analyzed by means of latent variable models. Methods such as *Partial Least Squares* (PLS) and *Principal Component Analysis* (PCA) have been widely used to tackle some of the mentioned problems. With a similar underlying rationale, *Factor Analysis* has also been considered (see e.g. Casa et al., 2022, for a recent work) since, allowing one to reduce the dimensionality of the data while focusing on a proper reconstruction of the correlation matrix, it seems particularly suitable for the framework. Recently, statistical and machine learning techniques have also been explored in order to relate spectral information to different milk traits (see e.g. Frizzarin et al., 2021a).

All these methods do not account for the peculiar structure of the spectral data and for the natural ordering among the variables, which can be considered by resorting to approaches pertaining to the functional data analysis setting (FDA; Ramsay and Silverman, 2005). In fact, even if Alsberg (1993) suggested that spectra should be represented as continuous functions of wavelengths, in this framework functional approaches have been to some extent overlooked until relatively recently (Saeys et al., 2008). Some works that it is worth mentioning, even if not necessarily focused on MIR spectral data, are the ones by Reiss and Ogden (2007); Morris et al. (2008); Zhao et al. (2012); Yang et al. (2016); Codazzi et al. (2022).

As briefly mentioned before, the varying degrees of smoothness of MIR spectroscopy data over their domain pose some challenges that need to be tackled when evaluating FDA strategies. Saeys et al. (2008) suggest to adopt a basis approach with unequally spaced knots, with knot placement driven by subject-matter knowledge on the properties of the analyzed material. In this work, we take a different approach by considering *trend filtering* as a building block of our approach (see Politsch et al., 2020, for a discussion in a similar framework).

1.1 Trend Filtering

Trend filtering is a signal reconstruction technique initially developed by [Kim et al. \(2009\)](#) and further studied, among others, by [Tibshirani \(2014\)](#). In the context of nonparametric regression, where data $\mathbf{y} = (y_1, y_2, \dots, y_p)^\top \in \mathbb{R}^p$ are supposed to be generated by the model $y_i = f_0(\omega_i) + \varepsilon_i$, $i = 1, \dots, p$, trend filtering solves the following empirical problem

$$\hat{\mathbf{f}} = \arg \min_{\mathbf{f} \in \mathbb{R}^p} \|\mathbf{y} - \mathbf{f}\|_2^2 + \lambda \|\mathbf{D}^{(k+1)} \mathbf{f}\|_1 \quad (1)$$

where $\mathbf{f} = (f(\omega_1), \dots, f(\omega_p))^\top$, $\mathbf{D}^{(k+1)} \in \mathbb{R}^{(p-k-1) \times p}$ is the discrete difference matrix of order $k + 1$, and $\lambda > 0$ is a tuning parameter. The resulting discretely estimated function $\hat{\mathbf{f}}$ has a number of interesting properties, the most important being its adaptivity to local features of the true underlying function f_0 . More precisely, the specification of the penalty yields a solution which, even if generally not sparse, exhibits a sparse $(k + 1)$ -th derivative. This behaviour resembles a spline function of degree k which possesses continuous derivatives up to order $k - 1$, while the k -th derivative is zero except for the points where polynomials meet, also known as *knots* of such spline. As shown in [Tibshirani \(2014\)](#), for $k = 1, 2$ the resulting estimated function is indeed a spline, while for $k > 2$ it is *close*, but not exactly equal, to a spline function with unequally spaced knots. The method is quite general thanks to the choice of k , e.g. with $k = 0$ one obtains a stepwise function with a first derivative that is different from zero only where jumps lie. In fact, given the form of $\mathbf{D}^{(1)}$, in this specific case the penalty becomes $\sum_{j=1}^{p-1} |f(x_j) - f(x_{j+1})|$ and the problem is equivalent to the Fused Lasso ([Tibshirani et al., 2005](#)). With $k = 1$ the second derivative is penalized, thus yielding an estimate that is piecewise linear. These and higher-order examples can be found in the original paper of [Tibshirani \(2014\)](#). A prominent instance is cubic trend filtering ($k = 3$) that allows to fit to the data something very similar to a cubic spline with unequally spaced knots. The further relevance of this approach can be appreciated also from another point of view; in the literature, several adaptive estimation procedures have been proposed, mainly focusing on finding good sets of spline knots (see e.g., [Dimatteo et al., 2001](#); [Zhou and Shen, 2001](#)). The trend filtering approach implicitly overcomes this problem since, by solving the minimization in (1) for a given λ , only a number $p_\lambda < p$ of knots are selected; the entire path spans a range of nested solutions without the need of a forward/backward knot search algorithm.

In this paper, after a brief description of the analyzed data in [Section 2](#), in [Section 3](#) we extend the main trend filtering concepts to functional regression with Gaussian scalar response, developing an estimator able to infer spatially inhomogeneous regression functions. We further investigate this modeling strategy in the case of a *partial* functional linear model, i.e. by including a set of scalar covariates and propose an extension intended for non-Gaussian response, as for example presence/absence or count data. Efficient estimation algorithms are presented in [Section 4](#), followed by a simulation study in [Section 5](#). In [Section 6](#) we present the result of the analysis on real data, while in [Section 7](#) we draw some final conclusions and remarks.

2 Mid-infrared spectroscopy data

In this study, we consider two different sets of mid-infrared spectroscopy data.

The first data set consists of a collection of 730 milk samples produced from 622 cows from different research herds in Ireland between August 2013 and August 2014. All the animals involved in the study were following a predominantly grass-based diet, with relevant heterogeneity in terms of number of parities and stage of lactation. Samples were collected during morning and evening milking and analyzed using a MilkoScan FT6000 (Foss Electronic A/S, Hillerød, Denmark). The resulting spectra consists of 1060 absorbance observations in the mid-infrared light region (see [Figure 1](#)). Furthermore, some additional information is available such as the date and the time (am/pm) of the milkings, the breed, the number of parities and the days in

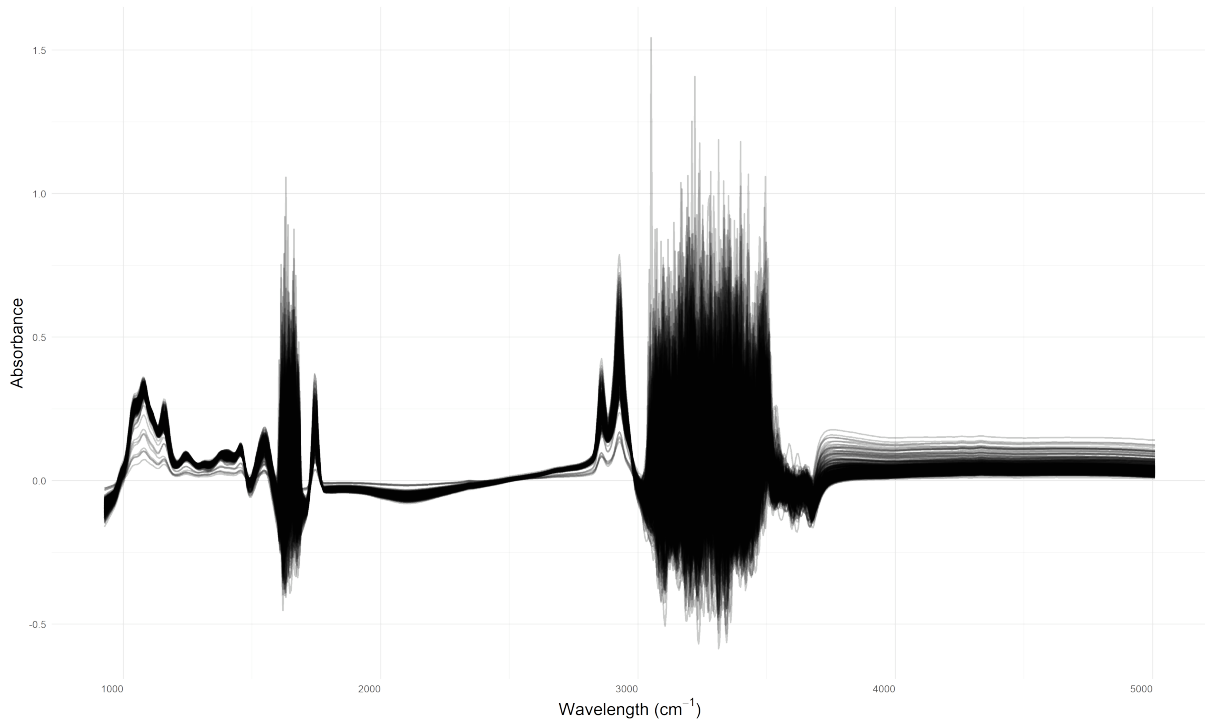


Figure 1: Mid-infrared spectra in the region from 925cm^{-1} to 5010cm^{-1} , corresponding to the first case study.

milk for all the cows involved in the study. Note that some milk related traits have been collected by means of wet chemistry techniques. Among these traits are included both technological, such as rennet coagulation time and heat stability, and protein related ones, as for example κ -casein and α_{S1} -casein. In the analyses reported in Section 6, we focus on the prediction of the κ -casein. Lastly, we retain only one observation per cow, thus working with 622 milk spectra. For a more complete description of the data collection process and of the data themselves, readers can refer to Visentin et al. (2015).

On the other hand, the second data set considered has been collected at the Teagasc Moorepark Dairy Research Farm (Fermoy, Co.Cork, Ireland), in an experiment designed by O’Callaghan et al. (2016b), which represents the first study of its kind in Ireland and, to the best of our knowledge, in the world. Further information on the experimental setting can be found in O’Callaghan et al. (2016a); O’Callaghan et al. (2017). The data consist of MIR spectra, comprising 1060 wavelengths in the region from 925cm^{-1} and 5010cm^{-1} , obtained by analyzing 4320 milk samples using a Pro-Foss FT6000 series instrument. A total number of 120 Holstein-Friesian cows have been involved in the study, and milked twice daily in the morning and in the afternoon in three consecutive years (2015, 2016 and 2017). The data collection scheme has been carried out in a balanced way, both in terms of the year and of the number of cattle’ parities. Moreover, we restrict our attention to the samples collected from May to August, since in the summer period there is the highest prevalence of grass growth. For each of the years considered, the cattle were randomly assigned to a specific dietary treatment for the entire lactation period. The treatment diets included grass (GRS), with cows maintained outdoors on a perennial ryegrass sward only, clover (CLV), consisting of perennial ryegrass with 20% white clover sward only, and total mixed ration (TMR), where cows were maintained indoors with nutrients combined in a single mix consisting of grass and maize silage and concentrates. In this work, given the strong compositional similarities between GRS and CLV diets, these two classes have been merged to create a general pasture-based diet group. As a consequence the final data set consists of 2931 samples from pasture-fed cattles and 1389 from TMR-fed ones. Lastly, some

additional information on fat, protein, and lactose content has been obtained by calibrating the FT6000 against wet chemistry results and is available for the milk samples considered.

3 Proposed methodology

Given the data $\mathcal{D} = \{X_i(\omega), y_i\}_{i=1}^n$, we assume that y_1, \dots, y_n are scalar values drawn from a Gaussian random variable $y_i|X_i(\omega) \sim N(\mu_i, \sigma^2)$ and $X_1(\omega), \dots, X_n(\omega)$ are realizations of a functional covariate. We model the conditional expected value of y_i as $\mathbb{E}(y_i|X_i(\omega)) = \mu_i = \int X_i(\omega)f(\omega)d\omega$ where $f(\omega)$ is an unknown regression function. This leads to the functional linear model

$$y_i = \int X_i(\omega)f(\omega)d\omega + \varepsilon_i,$$

with $\varepsilon_i \sim N(0, \sigma^2)$ being an additive noise term. There are several works in the functional data analysis literature devoted to estimation of this model, ranging from basis approaches (Ramsay and Silverman, 2005), penalized strategies (Crambes et al., 2009) and functional principal component representations (Yao et al., 2005). A complete review of different estimation methodologies is outside the scope of this work, and readers may refer to Morris (2015) for a general overview of such methods; however, here we spend some words on the penalization approach, which shares some features with our proposal.

Smoothing splines are the most popular tool in the family of penalized estimators. In the context of functional regression, given the data \mathcal{D} , they are obtained as the solution of the following optimization problem:

$$\hat{\mathbf{f}} = \arg \min_{\mathbf{f} \in \mathbb{R}^p} \|\mathbf{y} - \mathbf{X}\mathbf{f}\|_2^2 + \lambda \|\mathbf{D}^{(2)}\mathbf{f}\|_2^2, \quad (2)$$

where $\mathbf{y} = (y_1, \dots, y_n)^\top$ is the vector of scalar responses, $\mathbf{X} = (X_1(\omega), \dots, X_n(\omega))^\top$ is the matrix of functional data observed on a regular grid $\omega = (\omega_1, \dots, \omega_p)$ and $\mathbf{D}^{(2)}$ is the matrix of second order discrete differences. The approach is justified as a discrete counterpart of a certain variational problem and provides as a solution a natural cubic spline with knots at observation points, see Wahba (1990), Crambes et al. (2009) and Goldsmith et al. (2011) for details. The amount of penalization, managed by the tuning parameter λ , represents a trade-off between two extreme solutions, one being a completely wiggly interpolating function ($\lambda = 0$) and the other being a constant ($\lambda = \infty$). Despite being very intuitive and easy to implement, this estimator lacks the local adaptivity property, i.e. the resulting estimated curve is not able to capture the different levels of smoothness of the true function f . Therefore, we propose to rely on a different penalization strategy and estimate the regression curve by

$$\hat{\mathbf{f}} = \arg \min_{\mathbf{f} \in \mathbb{R}^p} \|\mathbf{y} - \mathbf{X}\mathbf{f}\|_2^2 + \lambda \|\mathbf{D}^{(k+1)}\mathbf{f}\|_1. \quad (3)$$

This expression represents a generalization of the trend filtering loss function, with the design matrix no longer being the $p \times p$ identity matrix (Tibshirani, 2014), but an $n \times p$ matrix of discretely observed functional data. The key difference between optimization problems (2) and (3) is that in the latter, thanks to the ℓ_1 -penalty applied on certain discrete derivative of f , we are able to estimate the regression function taking care of its local features. Indeed, similarly to the original trend filtering estimate, the function that minimizes (3) is equal (when $k = 1, 2$) or very similar (when $k > 2$) to a spline function with unequally spaced knots along its domain. Clearly, the smoothing splines approach, not being able to adapt to local features of the curve, either misses its smooth or its wiggly parts, depending on the selected degrees of freedom. This is a consequence of the regularization term which does not produce spatial heterogeneity nor knot selection. This makes the approach in (3) particularly appealing for spectroscopy data, where the effect of a functional covariate (e.g. the MIR spectrum) on a scalar variable (e.g. a material trait) can be studied with particular attention to local effects.

3.1 Extensions

In the current framework, when scalar covariates are available alongside the functional one, their inclusion in the modelling strategy can bring additional information useful to predict the response variable. More formally, in this setting we denote the observed data by $\mathcal{D} = \{X_i(\omega), y_i, \mathbf{z}_i\}_{i=1}^n$, with $\mathbf{z}_i = (z_{i1}, \dots, z_{ir})^\top$ being a set of r scalar covariates corresponding to the i -th observation. We then model the conditional expected value of y_i as $\mathbb{E}(y_i|X_i(\omega), \mathbf{z}_i) = \mu_i = \int X_i(\omega)f(\omega)d\omega + \sum_{j=1}^r z_{ij}\gamma_j$, where $\{\gamma_j\}_{j=1}^r$ are unknown regression coefficients. For such data structure, it is worth considering the partial functional linear model (Shin, 2009)

$$y_i = \int X_i(\omega)f(\omega)d\omega + \sum_{j=1}^r z_{ij}\gamma_j + \varepsilon_i.$$

Note that, if needed, the intercept can be easily included in the model as a constant scalar covariate. Following the trend filtering paradigm, we propose to estimate the function f and the vector $\boldsymbol{\gamma} = (\gamma_1, \dots, \gamma_r)^\top$ by solving the optimization problem

$$\hat{\boldsymbol{\theta}} = \arg \min_{\boldsymbol{\theta} \in \mathbb{R}^{p+r}} \|\mathbf{y} - \tilde{\mathbf{X}}\boldsymbol{\theta}\|_2^2 + \lambda \|\tilde{\mathbf{D}}^{(k+1)}\boldsymbol{\theta}\|_1, \quad (4)$$

where $\tilde{\mathbf{X}} = [\mathbf{X}|\mathbf{Z}] \in \mathbb{R}^{n \times (p+r)}$, $\mathbf{Z} = (\mathbf{z}_1, \dots, \mathbf{z}_n)^\top \in \mathbb{R}^{n \times r}$, $\boldsymbol{\theta} = (\mathbf{f}^\top, \boldsymbol{\gamma}^\top)^\top \in \mathbb{R}^{p+r}$ and $\tilde{\mathbf{D}}^{(k+1)} = [\mathbf{D}^{(k+1)}|\mathbf{0}_{(p-k-1) \times r}] \in \mathbb{R}^{(p-k-1) \times (p+r)}$. Note that, with this formulation, the penalty does not affect the parametric part of the model. When r is large, one can include an ℓ_1 -penalty for the vector $\boldsymbol{\gamma}$ in order to achieve sparsity in the estimated coefficients; see, for instance, Kong et al. (2016). Since the application presented in Section 6 involves a small set of covariates, this potential extension has not been pursued in this work.

An additional generalization of our proposal is required when assumption $y_i \sim N(\mu_i, \sigma^2)$ is not met because the scalar responses y_1, \dots, y_n are generated by some other distribution. For example, for count data, we can assume $y_i \sim \text{Poisson}(\lambda_i)$, and for presence/absence data $y_i \sim \text{Bernoulli}(\pi_i)$. In these settings, where a functional linear model is not adequate, a generalized functional linear model (James, 2002; Müller and Stadtmüller, 2005; Goldsmith et al., 2011) can be applied. In particular, we assume that $g(\mathbb{E}(y_i|X_i(\omega))) = g(\mu_i) = \int X_i(\omega)f(\omega)d\omega$, with $g(\cdot)$ being a suitably chosen link function. Now the empirical minimization problem is recasted as

$$\hat{\mathbf{f}} = \arg \min_{\mathbf{f} \in \mathbb{R}^p} L(\mathbf{y}; \mathbf{X}\mathbf{f}) + \lambda \|\mathbf{D}^{(k+1)}\mathbf{f}\|_1, \quad (5)$$

where the loss function $L(\mathbf{y}; \mathbf{X}\mathbf{f})$ depends upon the distribution of the response variable. The objective is now represented by a nonlinear function of the unknown parameter \mathbf{f} and its direct minimization is usually not straightforward. As a consequence, in Section 4 we present a clever modification of the proposed algorithm to deal with the modified loss appearing in (5). Lastly note that in the presence of explanatory scalar covariates and a non-Gaussian response, the last two specifications can be combined together by adjusting (5) as it has been done in equation (4) for problem (3).

Another potential extension would be to combine two (or more) penalties in the optimization problem. This allows to estimate functions that exhibit a complex behaviour, typically piecewise polynomials of different order. The loss function in this context is

$$\hat{\mathbf{f}} = \arg \min_{\mathbf{f} \in \mathbb{R}^p} \|\mathbf{y} - \mathbf{X}\mathbf{f}\|_2^2 + \lambda_1 \|\mathbf{D}^{(k+1)}\mathbf{f}\|_1 + \lambda_2 \|\mathbf{D}^{(\ell+1)}\mathbf{f}\|_1, \quad (6)$$

where k and ℓ are integers and λ_1, λ_2 are regularization parameters. This modification can be employed when additional scalar covariates are observed and/or when the distribution of the response is not Gaussian. In section 4 we will illustrate how to solve problem (6) with the same toolbox used for the other cases.

Algorithm 1 Wild bootstrap

Require: $\mathbf{X}, \mathbf{y}, \mathbf{D}, \lambda$

- 1: Compute the trend filtering estimate at the observed data points
- 2: Let $\hat{\epsilon}_i = y_i - \hat{y}_i = y_i - \sum_{j=1}^p X_i(\omega_j) \hat{f}(\omega_j)$
- 3: **for** b **in** $1:B$ **do**
- 4: **for all** i **do**
- 5: Define a bootstrap sample by sampling from the following distribution

$$y_i^* = \hat{y}_i + u_i^* \quad i = 1, \dots, n,$$

with u_i^* defined as in (7).

- 6: Let $\hat{\mathbf{f}}^{(b)} = (\hat{f}^{(b)}(\omega_1), \dots, \hat{f}^{(b)}(\omega_p))$ be the estimate from the bootstrap sample.
 - 7: Compute the bootstrap-based confidence bands as in (8).
-

3.2 Inference

In this section, we describe a strategy to build confidence intervals for most of the pointwise estimates introduced in the previous section. Given the complexity of functional regression models, inferential procedures have sometimes been overlooked, with the focus often being on pointwise estimation. Nonetheless, the introduced procedure represents a key component that improves the usability of the methodology in real world scenarios. In the case of the trend filtering framework, the construction of confidence intervals and confidence bands can be addressed via bootstrap procedures. Standard frequentist inference is not suitable, since the distribution of the trend filtering estimator is non-Gaussian, even when the observational noise is Gaussian (Politsch et al., 2020). Here we propose a Wild bootstrap procedure (Mammen, 1993), that is particularly appropriate in high-dimensional regression models when the noise distribution is unknown. Briefly, the idea behind the Wild bootstrap is to construct an auxiliary random variable with zero mean and unit variance (and ideally higher moments equal to 1). This random variable is then used to define a transformation of the observed residuals that gives a valid bootstrap sample (see Algorithm 1).

A classical choice for the auxiliary random variable is the two point distribution suggested in Mammen (1993), that is

$$u_i^* = \begin{cases} \hat{\epsilon}_i(1 + \sqrt{5})/2 & \text{with probability } (1 + \sqrt{5})/(2\sqrt{5}), \\ \hat{\epsilon}_i(1 - \sqrt{5})/2 & \text{with probability } (\sqrt{5} - 1)/(2\sqrt{5}). \end{cases} \quad (7)$$

Other examples are the Rademacher distribution, that takes values $1, -1$ with equal probability, the Uniform distribution on the interval $[-\sqrt{3}, \sqrt{3}]$, or various transformations of the Gaussian distribution (Mammen, 1993). In general, since it is not possible to define a random variable that has mean 0, variance 1, and all higher moments equal to 1, the different choices lead to different values for the third and the fourth moment. For instance, the third and fourth moments of the Rademacher distribution are 0 and 1, respectively, while the two point distribution defined above have third and fourth moments 1 and 2, respectively. The specific choice is generally driven by considerations on the symmetry of the observed residuals.

Given the full bootstrap estimate set $\{\hat{\mathbf{f}}^{(b)}\}_{b=1}^B$, for any $\alpha \in (0, 1)$, we can define a $(1 - \alpha)$ quantile-based pointwise variability band as

$$V_{1-\alpha}(f(\omega_j)) = \left(\hat{f}_{\alpha/2}(\omega_j), \hat{f}_{1-\alpha/2}(\omega_j) \right), \quad (8)$$

where

$$\hat{f}_\gamma(\omega_j) = \inf_g \left\{ g : \frac{1}{B} \sum_{b=1}^B \mathbb{I}(\hat{f}^{(b)}(\omega_j) \leq g) \geq \gamma \right\}, \quad \text{for all } j = 1, \dots, p.$$

4 Optimization procedure

In the literature, several algorithms for solving the original trend filtering problem have been proposed; see, among others, [Kim et al. \(2009\)](#), [Tibshirani \(2014\)](#) and [Tibshirani and Taylor \(2011\)](#). Some of these algorithms are not directly generalizable to our context, where the presence of the $n \times p$ data matrix \mathbf{X} makes the optimization task more challenging. To solve problem (3), we rely on the Alternating Direction Method of Multipliers (ADMM) framework and consider an extension of the approach by [Ramdas and Tibshirani \(2016\)](#) where a specialized acceleration scheme is proposed.

ADMM algorithms are a wide class of algorithms particularly useful for solving constrained problems of the form

$$\begin{aligned} & \text{minimize} && f(\boldsymbol{\alpha}) + g(\boldsymbol{\delta}), \\ & \text{subject to} && \mathbf{A}\boldsymbol{\alpha} + \mathbf{B}\boldsymbol{\delta} + \mathbf{c} = 0. \end{aligned} \tag{9}$$

A general ADMM algorithm proceeds by minimizing the augmented Lagrangian of (9). Since the objective function is separable, minimization can take place in an alternate fashion. ADMM approaches are largely used in penalized estimation schemes, which can often be recasted as in (9), leading to a faster optimization thanks to variable splitting. Specifically, the problem in (3) can be stated as

$$\begin{aligned} & \text{minimize} && \|\mathbf{y} - \mathbf{X}\boldsymbol{\alpha}\|_2^2 + \|\boldsymbol{\delta}\|_1, \\ & \text{subject to} && \mathbf{D}^{(k+1)}\boldsymbol{\alpha} - \boldsymbol{\delta} = 0. \end{aligned} \tag{10}$$

where $f(\boldsymbol{\alpha}) = \|\mathbf{y} - \mathbf{X}\boldsymbol{\alpha}\|_2^2$ is the ℓ_2 -loss and $g(\boldsymbol{\delta}) = \|\boldsymbol{\delta}\|_1$ the ℓ_1 -norm. As shown in [Boyd et al. \(2011\)](#), updates for the parameters are straightforward. In fact, since f is quadratic, the update step for $\boldsymbol{\alpha}$ has a least squares form and the $\boldsymbol{\delta}$ update amounts in soft-thresholding a given vector. Although these updating rules could be applied, an acceleration scheme for such problem is exploited. In fact, as demonstrated in [Ramdas and Tibshirani \(2016\)](#), a different parametrization of the ADMM can save computational time due to the existence of efficient algorithms for the constant-order trend filtering problem. The idea is to reformulate the problem as follows.

$$\begin{aligned} & \text{minimize} && \|\mathbf{y} - \mathbf{X}\boldsymbol{\alpha}\|_2^2 + \|\mathbf{D}^{(1)}\boldsymbol{\delta}\|_1, \\ & \text{subject to} && \mathbf{D}^{(k)}\boldsymbol{\alpha} - \boldsymbol{\delta} = 0. \end{aligned} \tag{11}$$

where $\mathbf{D}^{(1)}$ is the discrete difference matrix of order 1. The reader can verify the equivalence between problem (10) and problem (11). Hereafter, we derive the specialized parameter updates needed for the generic $t + 1$ iteration:

$$\boldsymbol{\alpha}^{t+1} = (\mathbf{X}^\top \mathbf{X} + \rho(\mathbf{D}^{(k)})^\top \mathbf{D}^{(k)})^{-1} (\mathbf{X}^\top \mathbf{y} + \rho(\mathbf{D}^{(k)})^\top (\boldsymbol{\delta}^t - \mathbf{u}^t)), \tag{12}$$

$$\boldsymbol{\delta}^{t+1} = \arg \min \|\mathbf{D}^{(k)}\boldsymbol{\alpha}^{t+1} + \mathbf{u}^t - \boldsymbol{\delta}^t\|_2^2 + \lambda/\rho \|\mathbf{D}^{(1)}\boldsymbol{\delta}^t\|_1, \tag{13}$$

$$\mathbf{u}^{t+1} = \mathbf{u}^t + \mathbf{D}^{(k)}\boldsymbol{\alpha}^{t+1} - \boldsymbol{\delta}^{t+1}. \tag{14}$$

The update for $\boldsymbol{\delta}$ is much more involved than a simple soft-thresholding and requires solving a new constant-order trend filtering problem, that is, a one-dimensional fused lasso problem. However, fast solutions are available by employing the dynamic programming solver by [Johnson \(2013\)](#) or the proposal by [Davies and Kovac \(2001\)](#) based on the taut string principle. [Ramdas and Tibshirani \(2016\)](#) showed the superiority of this specialized ADMM formulation over the classical one in terms of convergence rates: the single operation is more expensive than the one in the usual parametrization, but convergence is achieved in fewer iterations, leading to an overall gain in terms of computational time.

The parameter ρ is sometimes made adaptive by allowing a different value at each iteration to speed up the learning process. Using a varying ρ , one has to compute $(\mathbf{X}^\top \mathbf{X} + \rho^t \mathbf{D}^\top \mathbf{D})^{-1}$ at each iteration of the algorithm, and this can be prohibitive even for moderate dimensions. With a fixed ρ instead, one can precompute the quantity $(\mathbf{X}^\top \mathbf{X} + \rho \mathbf{D}^\top \mathbf{D})^{-1}$ that is never modified by the updating rules at the expense of some more iterations. In our implementation, we found this last approach faster and, in particular, we followed [Ramdas and Tibshirani \(2016\)](#) setting $\rho = \lambda$, which led to stable solutions. From a practical point of view, often the entire solution path is needed as a function of λ . In this case, a speed up is made by considering warm starts i.e., by starting the algorithm from the solution obtained for the previous value of the regularization parameter.

Lastly, note that slight modifications are needed in the presence of scalar covariates: the problem is stated as the minimization of $\|\mathbf{y} - \tilde{\mathbf{X}}\boldsymbol{\alpha}\|_2^2 + \|\mathbf{D}^{(1)}\boldsymbol{\delta}\|_1$ subject to $\tilde{\mathbf{D}}^{(k)}\boldsymbol{\alpha} - \boldsymbol{\delta} = 0$ and the updating rules are the same as ((12) – (14)) except for the substitution of $\tilde{\mathbf{X}}$ and $\tilde{\mathbf{D}}^{(k)}$ in place of \mathbf{X} and $\mathbf{D}^{(k)}$.

For the generalized functional linear model, we develop an iterative reweighted penalized least squares approach based on the alternation of a Newton step and an ADMM step. Specifically, problem (5) can be written as

$$\begin{aligned} & \text{minimize} && L(\mathbf{y}; \mathbf{X}\boldsymbol{\alpha}) + \|\mathbf{D}^{(1)}\boldsymbol{\delta}\|_1, \\ & \text{subject to} && \mathbf{D}^{(k)}\boldsymbol{\alpha} - \boldsymbol{\delta} = 0. \end{aligned} \tag{15}$$

In the first step of the algorithm, given the current estimate $\boldsymbol{\alpha}^t$ we approximate the generic loss function $L(\mathbf{y}; \mathbf{X}\boldsymbol{\alpha})$ around $\boldsymbol{\alpha}^t$ by a quadratic loss $\|\tilde{\mathbf{y}}^t - \tilde{\mathbf{X}}^t\boldsymbol{\alpha}\|_2^2$, where $\tilde{\mathbf{y}}^t = (\mathbf{W}^t)^{1/2}\mathbf{s}^t = (\mathbf{W}^t)^{1/2}(\mathbf{X}\boldsymbol{\alpha}^t + (\mathbf{V}^t)^{-1}(\mathbf{y} - \boldsymbol{\mu}^t))$ and $\tilde{\mathbf{X}}^t = (\mathbf{W}^t)^{1/2}\mathbf{X}$, building a penalized least squares problem. This step is intended as a Fisher scoring update. The quantities $\boldsymbol{\mu} = \mathbb{E}(\mathbf{y}|\mathbf{X})$, $\mathbf{V} = V(\boldsymbol{\mu})$ and $\mathbf{W} = V(\boldsymbol{\mu})^{-1}(g'(\boldsymbol{\mu}))^{-2}$ depend on the random variable characterizing the response. For example, if $y_i \sim \text{Bernoulli}(\pi_i)$ we have $\mu_i = \pi_i = \exp\{\int X_i(\omega)f(\omega)d\omega\}/(1+\exp\{\int X_i(\omega)f(\omega)d\omega\})$, $V(\mu_i) = \mu_i(1 - \mu_i)$, $g'(\mu_i) = 1/V(\mu_i)$ and $W_{ii} = V(\mu_i)$ while if $y_i \sim \text{Poisson}(\lambda_i)$ we have $\mu_i = \lambda_i = \exp\{\int X_i(\omega)f(\omega)d\omega\}$, $V(\mu_i) = \mu_i$, $g'(\mu_i) = 1/V(\mu_i)$ and $W_{ii} = V(\mu_i)$.

In the second step we solve the penalized problem by applying ADMM updates ((12) – (14)) until convergence, just by replacing \mathbf{X} with $\tilde{\mathbf{X}}^t$ and \mathbf{y} with $\tilde{\mathbf{y}}^t$, thus obtaining $\boldsymbol{\alpha}^{t+1}$. The two steps are repeated until some stopping criterion is achieved and the final estimator is obtained.

Lastly, note that it is possible to use the same machinery presented in this section for the multiple penalty approach too, by stacking the two matrices $\mathbf{D}^{(k+1)}$ and $\mathbf{D}^{(\ell+1)}$ to form $\tilde{\mathbf{D}}$, which will replace the difference matrix in the ADMM updates.

5 Simulation study

In this section, we assess the performance of the proposed methods by means of simulations. We first generate a sample of functional data $\{X_i(\omega)\}_{i=1}^n$ from a B-spline basis with 10 equispaced internal knots, drawing each coefficient from a standard normal distribution. The resulting functions are evaluated on an equispaced grid of $p = 100$ points in order to form the $n \times p$ matrix \mathbf{X} , and then kept fixed in all simulation repetitions. We define several scenarios that can be addressed with one of the methods previously described in the following way.

In scenario a), given the sample of functional data $\{X_i(\omega)\}_{i=1}^n$ we generate a sample of scalar responses from a Gaussian distribution $y_i \sim N(\mu_i, \sigma^2)$ where the expected value depends linearly on the functional covariate, i.e. $\mu_i = \int X_i(\omega)f(\omega)d\omega$. We set $n = 250$ and a signal-to-noise ratio equal to 4.

In scenario b), in addition to the functional data sample, we also consider a set of scalar covariates z_{1i}, \dots, z_{ri} for each observational unit. These covariates are generated from a standard Gaussian distribution and are independent of each other. Then, a sample of scalar responses is

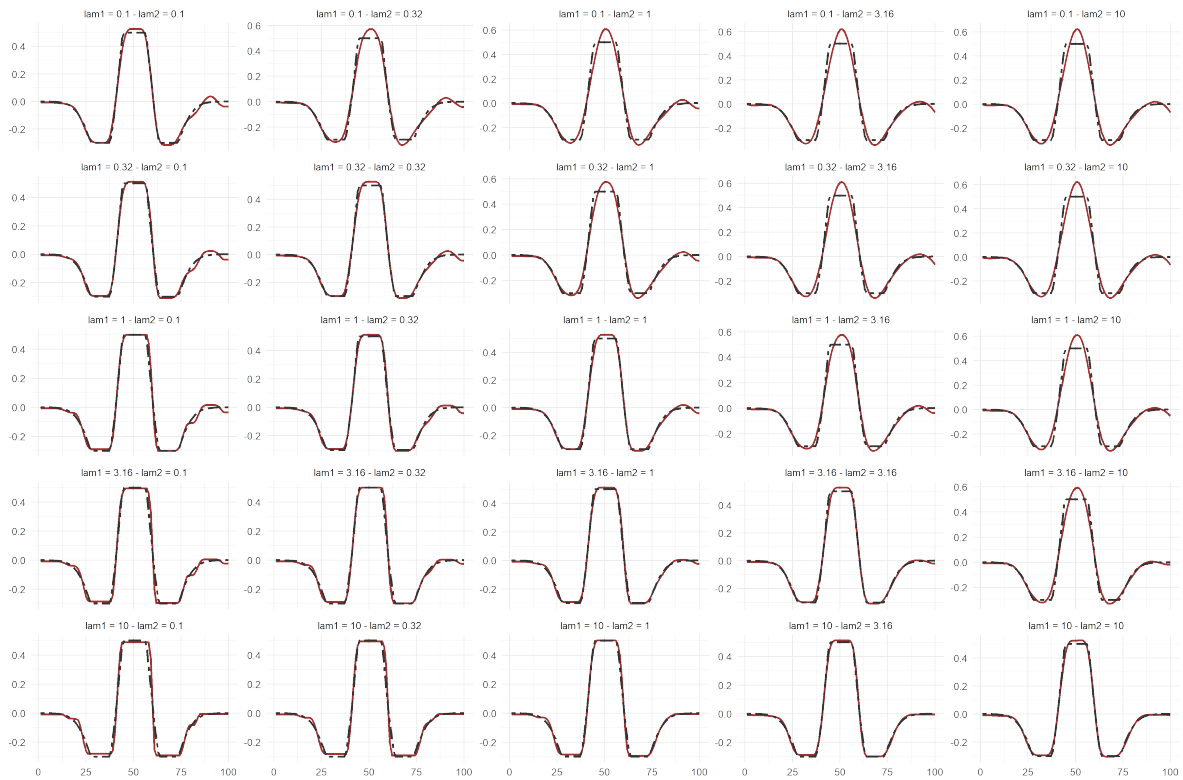


Figure 2: Estimated functional coefficient for $f_3(\omega)$, with different combinations of (λ_1, λ_2) in the mixed penalty case $k = 0, l = 3$. The dashed-black lines correspond to the true function, while the solid-red lines correspond to estimates. From top to bottom, the estimated functional coefficient approaches a piecewise-constant function; from left to right, it approaches a cubic function.

Table 1: Average Integrated Mean Squared Error (MISE) and its standard error (in parentheses) over 100 repetitions for the estimation of three regression functions (details in the text). *TF-4*: Trend filtering with penalization on fourth derivative only; *TF-1*: Trend filtering with penalization on the first derivative only; *MTF*: Trend filtering with penalization on both fourth and first derivative; *SPL*: Penalized splines as in Goldsmith et al. (2011).

Function	$f_1(\omega)$	$f_2(\omega)$	$f_3(\omega)$
Scenario a)			
<i>TF-4</i>	0.335 (0.401)	0.123 (0.173)	0.265 (0.073)
<i>TF-1</i>	1.969 (1.821)	2.120 (0.680)	0.595 (0.339)
<i>MTF</i>	0.588 (0.514)	0.297 (0.296)	0.184 (0.081)
<i>SPL</i>	0.669 (0.666)	0.207 (0.860)	0.357 (0.405)
Scenario b)			
<i>TF-4</i>	0.382 (0.434)	0.139 (0.189)	0.269 (0.083)
<i>TF-1</i>	1.584 (0.335)	2.035 (0.189)	0.561 (0.069)
<i>MTF</i>	0.513 (0.395)	0.302 (0.299)	0.194 (0.083)
<i>SPL</i>	1.101 (1.014)	0.221 (0.941)	0.368 (0.477)
Scenario c)			
<i>TF-4</i>	2.051 (1.861)	0.822 (0.586)	0.680 (0.472)
<i>TF-1</i>	4.334 (2.180)	2.705 (1.091)	0.907 (0.363)
<i>MTF</i>	3.713 (2.386)	1.165 (0.974)	0.579 (0.298)
<i>SPL</i>	2.698 (1.122)	0.908 (1.676)	0.630 (0.366)

obtained from a Gaussian distribution $y_i \sim N(\mu_i, \sigma^2)$ where the expected value depends linearly on the functional and scalar covariates, i.e. $\mu_i = \int X_i(\omega)f(\omega)d\omega + \sum_{j=1}^r z_{ji}\gamma_j$. We set $n = 250$, $r = 5$, $\gamma = (2, -1, 1, 0, 0)$ and a signal-to-noise ratio equal to 4.

In scenario c), given the functional data sample, we generate scalar responses from a Bernoulli distribution $y_i \sim \text{Bernoulli}(\pi_i)$ where $g(\pi_i) = \text{logit}\{\pi_i\}$ depends linearly on the functional covariate, i.e. $\text{logit}\{\pi_i\} = \int X_i(\omega)f(\omega)d\omega$. We set $n = 250$.

We combine each described scenario with three different specifications of the unknown regression function $f(\omega)$. In detail, $f_1(\omega)$ is a piecewise cubic function in $[0, 1]$ built from a cubic B-spline basis with 3 internal knots at 0.2, 0.75 and 0.9, $f_2(\omega)$ is the classical mexican hat function

$$f_2(\omega) = (1 - \omega^2)\exp\{-\omega^2/2\} \quad \text{for } \omega \in [-5, 5],$$

and $f_3(\omega)$ is the same function with truncated peaks

$$f_3(\omega) = \begin{cases} f_2(\omega) & \text{if } f_2(\omega) \in [-0.3, 0.5], \\ 0.5 & \text{if } f_2(\omega) > 0.5, \\ -0.3 & \text{if } f_2(\omega) < -0.3. \end{cases}$$

All functions are evaluated on the same equispaced grid of $p = 100$ points used to generate $\{X_i(\omega)\}_{i=1}^n$.

For all the $B = 100$ synthetic samples generated, we estimate the regression parameters with the trend filtering approach, penalizing the fourth derivative (*TF-4*), the first derivative (*TF-1*) and both of them (*Mixed-TF*). For comparison purposes we also employ the spline method (*SPL*) outlined in Goldsmith et al. (2011) penalizing the second derivative of the function. The tuning parameters for all the methods have been selected using a separate validation set. In Table 1 we present for our methods and the spline estimator the value of the Integrated Mean

Squared Error (MISE) defined as

$$\text{MISE}(\hat{f}) = \int \{f(\omega) - \hat{f}(\omega)\}^2 d\omega,$$

evaluated on the finite grid ω , averaged over all simulation repetitions, and its standard error (in parenthesis). The proposed approach shows superior performance in all the combinations of functions and scenarios considered, when compared to the spline methodology. In fact, this latter strategy is not well suited in situations where the regression function is spatially heterogeneous. Moreover we observe that, among the different specifications of the trend filtering, the one penalizing the fourth derivative achieves the best results in estimating $f_1(\omega)$ and $f_2(\omega)$, in all considered scenarios. Unfortunately, penalizing the first derivative does not lead to satisfactory results, for two main reasons: the estimated regression function is not continuous, against what is commonly assumed in functional data analysis, and the estimation error is large due to inherent smoothness of the considered unknowns. However, adding the first derivative penalization to the plain trend filtering of order four leads to an improved performance if the regression function is particularly complex, as in the case of $f_3(\omega)$. To elucidate the behaviour of double penalization in this scenario, in Figure 2 we graphically depict the unknown function and several estimates based on different values of the parameter $\lambda = (\lambda_1, \lambda_2)$. Starting from the upper left corner where the impact of regularization is the lowest, we see that increasing λ_1 keeping λ_2 fixed, leads to almost piecewise constant solutions. By contrast, increasing λ_2 while keeping λ_1 fixed, leads to almost piecewise cubic functions. However, since $f_3(\omega)$ exhibits both features, a better reconstruction is obtained by combining the two penalties, as can be appreciated in the lower right corner of the figure. Lastly, note that this specification automatically includes the “marginal” models with only one of the two derivative penalized.

6 Applications to milk spectral data

In the following, the proposed method is applied to the first set of data introduced in Section 2. Following suggestions from the literature, prior to running the analyses a variables aggregation step has been performed. In fact, it has been pointed out (see e.g., [Murphy et al., 2010](#)) that the aggregation of adjacent wavelengths implies almost negligible losses in terms of information and predictive abilities. This is coherent with the idea that, when dealing with spectra, the strong correlations among wavelengths allow to work on data with slightly lower resolution while retaining most of the informative content. Accordingly, we aggregate four adjacent wavelengths, to reduce the overall computational cost, resulting in a dataset with $n = 622$ milk spectra and $p = 264$ wavelengths.

As briefly mentioned in Section 2, in the regression framework the proposed method has been used to predict the κ -casein content in the milk samples. The actual observed values for the response variable, expressed in grams per liter of milk, were collected using reverse-phase high performance liquid chromatography (HPLC), with an adaptation of the methodology considered in [Visser et al. \(1991\)](#). This technology is known to be expensive and time-consuming and is not considered suitable for modern large-scale applications; therefore, the calibration of statistical tools, used in conjunction with infrared spectroscopy, can be highly beneficial for research in the dairy framework and for the dairy production systems.

κ -casein has been selected as the milk trait to be predicted as it is one of the major components of milk, playing an essential role in cheese production systems, affecting both cheese yield and its characteristics ([Wedholm et al., 2006](#)). Moreover, κ -casein is also used as a food additive and it generally represents an important economic factor whose timely and precise prediction might increase the efficiency of the dairy production chain. For these reasons, milk casein content is nowadays also considered as one of the determinants to estimate the breeding values of the animals, inspiring research lines on genetic control and selective breeding ([Bittante](#)

Table 2: Estimated coefficients, and 95% confidence intervals, for the scalar covariates.

Covariate	Lower (0.025)	Estimate	Upper (0.975)
Intercept	0.257	0.438	0.627
Spring	-0.222	-0.133	-0.038
Summer	-0.075	-0.019	0.026
Milk time (morning)	-0.186	-0.129	-0.074
Parity (2)	-0.061	-0.019	0.030
Parity (3)	-0.043	0.004	0.052
DIM	-0.001	-0.000	0.000

and Cecchinato, 2013; Bittante et al., 2022). Exploratory analysis of this variable revealed a strong asymmetric behaviour of the empirical distribution. For this reason, we considered as a response variable for our model the logarithm of κ -casein.

In this section, the model in (6) has been considered, with $k = 3$ and $l = 0$, thus penalizing the fourth and the first derivative, respectively. This choice can be justified by the assumption of a regression function that is smooth in some parts of the domain and flat in some others. Note, as mentioned in section 5, that the marginal formulations with penalization only on the fourth or on the first derivative are included as limiting models. The hyperparameters λ_1 and λ_2 , which control the strenght of the penalty, have been selected resorting to a cross-validation scheme. In conjunction with the spectral variables, we consider also some scalar covariates, as per the extension of the model outlined in Section 3.1; in particular, information on the season when the milk samples have been collected, the milking time (morning or afternoon milking), the number of cows' parities and the number of days an animal has been milking in the current lactation (days in milk). This implies the presence of $r = 6$ additional scalar variables, with a total of 270 covariates. The estimated regression function, together with the inferential results obtained by means of the procedure introduced in Section 3.2, are visually reported in Figure 3, while the results concerning the scalar variables are shown in Table 2.

The method shows high prediction accuracy, with a cross-validated mean square prediction error equal to 0.04986. The result has been additionally compared with a PLS-based regression approach, unarguably representing the state-of-the-art when working with infrared spectroscopy data, which resulted in a cross-validated mean square prediction error of 0.05457.

As mentioned, our proposal introduces other relevant strength points while showing improved predictive performance. First, it respects and preserves the functional nature of the data, without mapping them into lower-dimensional latent spaces. Consequently, it provides richer insights on the studied phenomenon and, generally speaking, an easier interpretation of the results; this potentially sheds light on the chemical factors which are the main determinants of casein content in milk. In fact, a thorough analysis of the results depicted in Figure 3 highlights some interesting behaviours. First of all, the inferential routine outlined in Section 3.2, allows to detect some spectral regions which are considered to be uninformative for the determination of the κ -casein content in the milk. For instance, our method considers as uninformative the spectral regions from 1619 cm^{-1} to 1673 cm^{-1} and from 3069 cm^{-1} to 3663 cm^{-1} . In literature these highly-noisy regions are designated as water absorption areas, usually considered as uninformative, thus removed from the data prior to the analyses (Rutten et al., 2011). Nonetheless, the determination of these regions is still controversial and not unambiguous, as it can be influenced by spectrometer specific characteristics. Interestingly, our method marks as uninformative more wavelengths being adjacent to these highly noisy regions; this is coherent with practitioners' experiences which often point out that water may influence larger portions of the spectra, with respect to the ones suggested in the literature.

Focusing on the variables regarded as significant, it has to be noted that the proposal suggests that κ -casein can be predicted using a relatively small portion of the infrared spectrum. This is

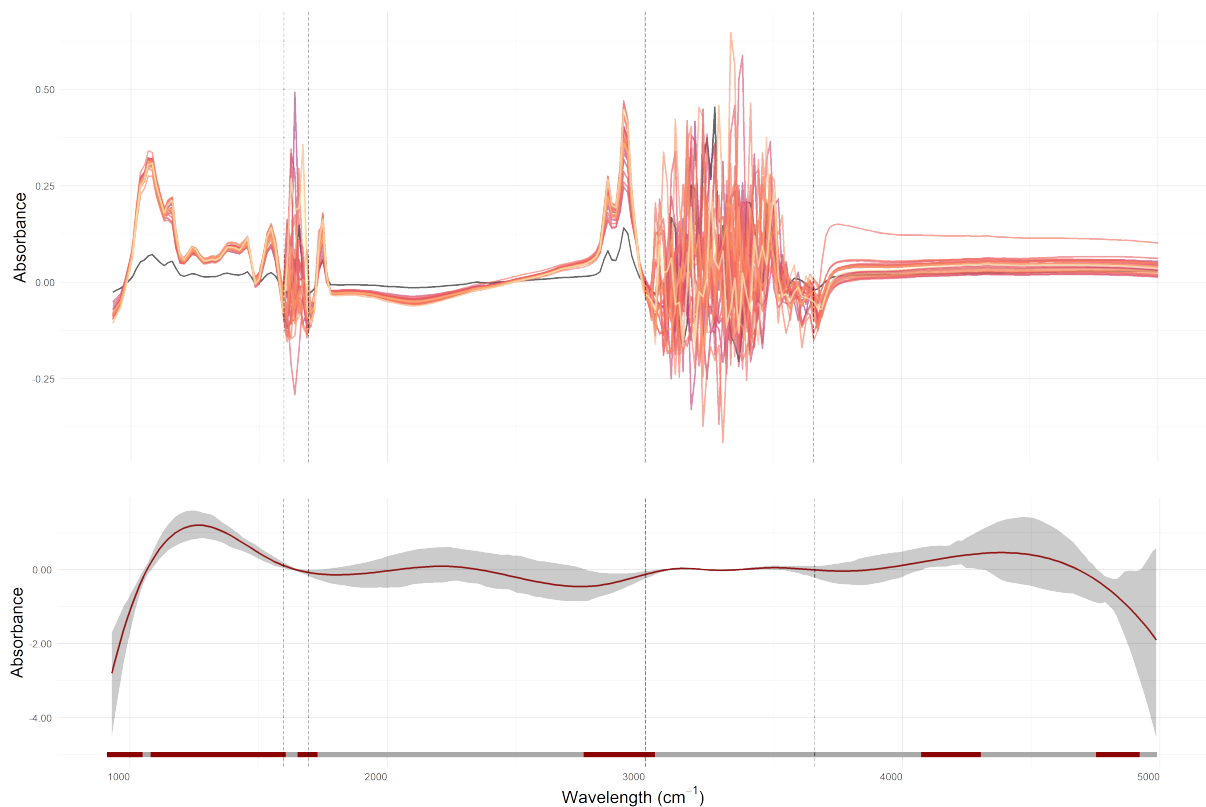


Figure 3: Top: Sample of 25 spectra, with dark (light) colors corresponding to low (high) values of κ -casein. Bottom: Estimated functional coefficient with 95% bootstrap bands. The regions that do not contain zero are highlighted in red in the bottom line.

consistent with the results obtained in [Frizzarin et al. \(2021a\)](#) where standard predictive tools displayed good performances exploiting fewer wavelengths, with respect to the ones used to predict other milk proteins and technological traits. These indications are particularly important for the dairy industry, where there is an increasing demand for cheaper and potentially portable instruments, scanning only relevant portions of the spectrum.

A proper interpretation of the specific peaks shown in the estimated regression function is complex since, for composite materials as milk, chemical constituents have absorption peaks at different wavelengths which often overlap ([Soyeurt et al., 2006](#)). Nonetheless, some interesting behaviours can be highlighted. In general, we see a strong influence for the wavelengths in the so called *fingerprnt region*, below 1400 cm^{-1} ([Hewavitharana and van Brakel, 1997](#)); this region is often regarded as highly informative for the analysis of proteinaceous material as here chemical bonds related to amide groups are formed ([Van Der Ven et al., 2002](#)). Coherently, being κ -casein a protein, our method flags as influential, and with a positive effect on the κ -casein concentration, those wavelengths around 1550 cm^{-1} and 1250 cm^{-1} which are associated with amide II and amide III bands ([De Marchi et al., 2009](#)). In the region around 1100 cm^{-1} and between 1200 cm^{-1} and 1300 cm^{-1} , the peaks often depend on the phosphate bands; interestingly, phosphorus in milk occurs only in casein and not in whey proteins ([Hewavitharana and van Brakel, 1997](#)) and our method seems to be able to detect the importance of these areas.

Lastly, some insights can be obtained by inspecting the results for the scalar covariates. For example, milk samples collected in spring appear to have a significant decrease in terms of κ -casein concentration; knowing that cows calve in the first months of the year, this is consistent with the suggestions in [Sørensen et al. \(2003\)](#) where it is stated that casein concentration is usually lower after calving. Moreover, [Quist et al. \(2008\)](#); [Forsbäck et al. \(2010\)](#) showed that casein content is higher for afternoon and evening milkings, with respect to the morning ones;

as it can be seen in Table 2, this is confirmed by our results.

Generally speaking, the devised procedure is capable of adequately predict the content of κ -casein in milk while, at the same time, paving the way for a convenient interpretation of the results, which is often more cumbersome when different predictive tools are considered. Finally, it should be noted that interpretation must be paired, as it might be enriched, by a close cooperation with an expert in the dairy and animal science framework.

6.1 Application to cow dietary treatments

In this section, one of the extension discussed in Section 3.1, is considered to analyze the second datasets introduced in Section 2. More specifically, assuming that the response variable arises from a Bernoulli distribution, we employ the proposed strategy to predict the cows' dietary treatment, relying only on the spectral information. Coherently with the application in the previous section, a wavelength aggregation step has been performed. Moreover, consistently with Frizzarin et al. (2021b), some outlying spectra have been removed. This results in a set of data with $n = 4261$ spectra, 2893 from pasture-fed cows and 1368 from TMR-fed ones, and $p = 264$ measured wavelengths.

Hereafter, model (5) has been employed; in particular we considered $k = 0$, therefore penalizing the first derivative, with the loss function adequately chosen to accommodate the binary nature of the response variable. The hyperparameter λ has been selected again by cross-validation. The application of our method produces highly satisfactorily performances, resulting in a cross-validation missclassification error equal to 2.98%. This result has been again compared with the one obtained by means of a PLS-based discriminant analysis strategy, which produced a similar cross-validated error equal to 2.60%. This provides a strong indication about the suitability of our proposal, also when considered for classification purposes.

Note that the extension to model (5) of the procedure outlined in Section 3.2 is not trivial. Nevertheless, even if it is not possible to draw formal inferential conclusions on the estimated functional coefficient, a closer inspection of the result allows us to obtain relevant insights, which can be further explored and integrated with subject-matter knowledge. Firstly, the penalization on the first derivative allows one to obtain an estimated functional coefficient being flat and equal to zero, or having negligible magnitude, for the highly noisy spectral regions from 1604 cm^{-1} to 1712 cm^{-1} , and from 3039 cm^{-1} to 3810 cm^{-1} , which strongly overlaps with the water absorption areas, deemed irrelevant for discrimination. Small discrepancies with the results obtained in the previous section highlight how the proposed method could represent a completely data-driven and application-oriented way to detect uninformative spectral regions. Further inspection of the most relevant wavelengths leads to coherent indications, with respect to those available in the literature (see e.g., Frizzarin et al., 2021b). For example, the *fingerprint region* is again useful to discriminate between diets. Moreover, wavelengths between 2854 cm^{-1} and 2977 cm^{-1} seems to have a strong impact on the feeding regimens classification, thus agreeing with the suggestions in De Marchi et al. (2011); Lefevre and Subirade (2000) where it is highlighted that this region is often used to estimate the milk fatty acid composition, which is in turn known to be highly correlated with the dietary treatment.

Concluding the proposed classification tool, while respecting and preserving the functional nature of the data, is able to outperform state-of-the-art discriminative methods. Moreover, the inspection of the estimated coefficients allows us to gain relevant insights from a chemical standpoint, which might deserve further exploration from experts in the field.

7 Conclusions and future directions

In this work, we presented an adaptive functional framework for spectroscopy data, that stems from the trend filtering literature. The proposed regression method is characterized by high

flexibility and adaptivity with respect to the complexity of the underlying data generating process. In particular, the method is capable of capturing different degrees of regularity of the slope function, while accounting for the high dimensionality and strong correlation among the wavelengths thanks to the ℓ_1 -regularization. The estimation is supported by a fast optimization procedure that leverages on the alternating direction method of multipliers framework, with a specialized acceleration scheme which provides superior convergence rates. The method is suitable for both Gaussian and non-Gaussian responses, and allows for the inclusion of scalar covariates, whose addition is often overlooked in the spectroscopy framework even if it might lead to better predictive performances. Moreover, the estimation strategy is enriched by a newly developed inferential procedure which allows to draw formal conclusions both on the functional and the scalar component. These are obtained with a nonparametric bootstrap approach, i.e. the wild bootstrap, that is particularly appropriate in high-dimensional regression models where the noise distribution is unknown.

The high adaptivity and the availability of inferential procedure are key features to enhance not only the interpretability of the results, but also their usability in real world scenarios. Indeed, spectroscopy data present peculiar statistical challenges, in particular intrinsic high-dimensionality of the inputs and strong correlation structures among the wavelengths. It is therefore paramount, from a practical perspective, to have a viable and interpretable tool that allows to carry out inference on specific regions of the spectrum, in order to gain relevant knowledge on specific properties of the samples (e.g. κ -casein content) or to highlight differences due to external factors (e.g. dietary treatments).

The proposed methodology showed satisfactory performance in simulations and, more importantly, very promising results in the two spectroscopy-based data analyses. In terms of prediction accuracy, the results were either superior or comparable to the ones obtained by means of state-of-the-art techniques. In terms of inference, the flexibility of the model allowed a correct identification of the highly-noisy water absorption areas, without the necessity to remove such portions of the data prior to the analysis. Moreover, in both the regression and classification framework, informative peaks (e.g., those in the fingerprint region) were highlighted, providing interesting insights into which spectral regions affect certain properties of milk. The inclusion of covariates has also constituted a relevant advantage that resulted in interesting observations on the effect, for example, of the seasonality. It should be stressed that, even if the proposed methodology has been applied to MIR spectroscopy data, it may be extended to other data sharing similar features.

A first direction for future research might be the development of inferential procedures for the non-Gaussian response cases. This would solidify the interpretability of the proposed methods even further, for instance in the classification framework. Moreover, this represents a particularly stimulating open problem, that might be approached via appropriate generalization of the nonparametric bootstrap procedures. Another possible extension could be the introduction of more complex penalties, that would allow the applicability of the method to a wider range of problems.

Acknowledgements

This publication has emanated from research conducted with the financial support of Science Foundation Ireland (SFI) and the Department of Agriculture, Food and Marine on behalf of the Government of Ireland under grant number (16/RC/3835).

References

Alsberg, B. K. (1993). Representation of spectra by continuous functions. *Journal of Chemometrics*, 7(3):177–193.

- Beer, A. (1852). Bestimmung der absorption des rothen lichts in farbigen flüssigkeiten. *Annalen der Physik Chemie*, 162:78–88.
- Berzaghi, P. and Riovanto, R. (2009). Near infrared spectroscopy in animal science production: principles and applications. *Italian Journal of Animal Science*, 8(sup3):39–62.
- Bittante, G. and Cecchinato, A. (2013). Genetic analysis of the fourier-transform infrared spectra of bovine milk with emphasis on individual wavelengths related to specific chemical bonds. *Journal of Dairy Science*, 96(9):5991–6006.
- Bittante, G., Patel, N., Cecchinato, A., and Berzaghi, P. (2022). Invited review: A comprehensive review of visible and near-infrared spectroscopy for predicting the chemical composition of cheese. *Journal of Dairy Science*.
- Boyd, S., Parikh, N., Chu, E., Peleato, B., and Eckstein, J. (2011). Distributed optimization and statistical learning via the alternating direction method of multipliers. *Foundations and Trends® in Machine Learning*, 3(1):1–122.
- Casa, A., O’Callaghan, T. F., and Murphy, T. B. (2022). Parsimonious bayesian factor analysis for modelling latent structures in spectroscopy data. *The Annals of Applied Statistics*, 16(4):2417–2436.
- Codazzi, L., Colombi, A., Gianella, M., Argiento, R., Paci, L., and Pini, A. (2022). Gaussian graphical modeling for spectrometric data analysis. *Computational Statistics & Data Analysis*, page 107416.
- Crambes, C., Kneip, A., and Sarda, P. (2009). Smoothing splines estimators for functional linear regression. *The Annals of Statistics*, 37(1):35 – 72.
- Davies, P. L. and Kovac, A. (2001). Local Extremes, Runs, Strings and Multiresolution. *The Annals of Statistics*, 29(1):1 – 65.
- De Marchi, M., Bonfatti, V., Cecchinato, A., Di Martino, G., and Carnier, P. (2009). Prediction of protein composition of individual cow milk using mid-infrared spectroscopy. *Italian Journal of Animal Science*, 8(sup2):399–401.
- De Marchi, M., Penasa, M., Cecchinato, A., Mele, M., Secchiari, P., and Bittante, G. (2011). Effectiveness of mid-infrared spectroscopy to predict fatty acid composition of brown swiss bovine milk. *Animal*, 5(10):1653–1658.
- De Marchi, M., Toffanin, V., Cassandro, M., and Penasa, M. (2014). Invited review: Mid-infrared spectroscopy as phenotyping tool for milk traits. *Journal of Dairy Science*, 97(3):1171–1186.
- Dimatteo, I., Genovese, C. R., and Kass, R. E. (2001). Bayesian curve-fitting with free-knot splines. *Biometrika*, 88(4):1055–1071.
- Forsbäck, L., Lindmark-Månsson, H., Andrén, A., Åkerstedt, M., Andrée, L., and Svennersten-Sjaunja, K. (2010). Day-to-day variation in milk yield and milk composition at the udder-quarter level. *Journal of dairy science*, 93(8):3569–3577.
- Frizzarin, M., Gormley, I., Berry, D., Murphy, T., Casa, A., Lynch, A., and McParland, S. (2021a). Predicting cow milk quality traits from routinely available milk spectra using statistical machine learning methods. *Journal of Dairy Science*, 104(7):7438–7447.
- Frizzarin, M., O’Callaghan, T. F., Murphy, T. B., Hennessy, D., and Casa, A. (2021b). Application of machine-learning methods to milk mid-infrared spectra for discrimination of cow milk from pasture or total mixed ration diets. *Journal of Dairy Science*, 104(12):12394–12402.

- Goldsmith, J., Bobb, J., Crainiceanu, C. M., Caffo, B., and Reich, D. (2011). Penalized functional regression. *Journal of Computational and Graphical Statistics*, 20(4):830–851.
- Hewavitharana, A. K. and van Brakel, B. (1997). Fourier transform infrared spectrometric method for the rapid determination of casein in raw milk. *Analyst*, 122(7):701–704.
- James, G. M. (2002). Generalized linear models with functional predictors. *Journal of the Royal Statistical Society: Series B (Statistical Methodology)*, 64(3):411–432.
- Johnson, N. A. (2013). A dynamic programming algorithm for the fused lasso and l_0 -segmentation. *Journal of Computational and Graphical Statistics*, 22(2):246–260.
- Keller, L. P., Bajt, S., Baratta, G. A., Borg, J., Bradley, J. P., Brownlee, D. E., Busemann, H., Brucato, J. R., Burchell, M., Colangeli, L., et al. (2006). Infrared spectroscopy of comet 81p/wild 2 samples returned by stardust. *Science*, 314(5806):1728–1731.
- Kim, S.-J., Koh, K., Boyd, S., and Gorinevsky, D. (2009). l_1 trend filtering. *SIAM Review*, 51(2):339–360.
- Kong, D., Xue, K., Yao, F., and Zhang, H. H. (2016). Partially functional linear regression in high dimensions. *Biometrika*, 103(1):147–159.
- Lefevre, T. and Subirade, M. (2000). Interaction of β -lactoglobulin with phospholipid bilayers: a molecular level elucidation as revealed by infrared spectroscopy. *International journal of biological macromolecules*, 28(1):59–67.
- Mammen, E. (1993). Bootstrap and wild bootstrap for high dimensional linear models. *The Annals of Statistics*, 21(1):255–285.
- McParland, S. and Berry, D. (2016). The potential of fourier transform infrared spectroscopy of milk samples to predict energy intake and efficiency in dairy cows. *Journal of Dairy Science*, 99(5):4056–4070.
- Morris, J. S. (2015). Functional regression. *Annual Review of Statistics and Its Application*, 2(1):321–359.
- Morris, J. S., Brown, P. J., Herrick, R. C., Baggerly, K. A., and Coombes, K. R. (2008). Bayesian analysis of mass spectrometry proteomic data using wavelet-based functional mixed models. *Biometrics*, 64(2):479–489.
- Murphy, T. B., Dean, N., and Raftery, A. E. (2010). Variable selection and updating in model-based discriminant analysis for high dimensional data with food authenticity applications. *The Annals of Applied Statistics*, 4(1):396.
- Müller, H.-G. and Stadtmüller, U. (2005). Generalized functional linear models. *The Annals of Statistics*, 33(2):774 – 805.
- O’Callaghan, T. F., Mannion, D. T., Hennessy, D., McAuliffe, S., O’Sullivan, M. G., Leeuwendaal, N., Beresford, T. P., Dillon, P., Kilcawley, K. N., Sheehan, J. J., et al. (2017). Effect of pasture versus indoor feeding systems on quality characteristics, nutritional composition, and sensory and volatile properties of full-fat cheddar cheese. *Journal of Dairy Science*, 100(8):6053–6073.
- O’Callaghan, T. F., Faulkner, H., McAuliffe, S., O’Sullivan, M. G., Hennessy, D., Dillon, P., Kilcawley, K. N., Stanton, C., and Ross, R. P. (2016a). Quality characteristics, chemical composition, and sensory properties of butter from cows on pasture versus indoor feeding systems. *Journal of Dairy Science*, 99(12):9441–9460.

- O’Callaghan, T. F., Hennessy, D., McAuliffe, S., Kilcawley, K. N., O’Donovan, M., Dillon, P., Ross, R. P., and Stanton, C. (2016b). Effect of pasture versus indoor feeding systems on raw milk composition and quality over an entire lactation. *Journal of Dairy Science*, 99(12):9424–9440.
- Petrich, W. (2001). Mid-infrared and raman spectroscopy for medical diagnostics. *Applied Spectroscopy Reviews*, 36(2-3):181–237.
- Politsch, C. A., Cisewski-Kehe, J., Croft, R. A., and Wasserman, L. (2020). Trend filtering–i. a modern statistical tool for time-domain astronomy and astronomical spectroscopy. *Monthly Notices of the Royal Astronomical Society*, 492(3):4005–4018.
- Porep, J. U., Kammerer, D. R., and Carle, R. (2015). On-line application of near infrared (nir) spectroscopy in food production. *Trends in Food Science & Technology*, 46(2):211–230.
- Quist, M., LeBlanc, S., Hand, K., Lazenby, D., Miglior, F., and Kelton, D. (2008). Milking-to-milking variability for milk yield, fat and protein percentage, and somatic cell count. *Journal of Dairy Science*, 91(9):3412–3423.
- Ramdas, A. and Tibshirani, R. J. (2016). Fast and flexible admm algorithms for trend filtering. *Journal of Computational and Graphical Statistics*, 25(3):839–858.
- Ramsay, J. O. and Silverman, B. W. (2005). *Functional data analysis*. Springer, New York.
- Reid, L. M., O’donnell, C. P., and Downey, G. (2006). Recent technological advances for the determination of food authenticity. *Trends in Food Science & Technology*, 17(7):344–353.
- Reiss, P. T. and Ogden, R. T. (2007). Functional principal component regression and functional partial least squares. *Journal of the American Statistical Association*, 102(479):984–996.
- Rutten, M., Bovenhuis, H., Heck, J., and van Arendonk, J. (2011). Prediction of β -lactoglobulin genotypes based on milk fourier transform infrared spectra. *Journal of dairy science*, 94(8):4183–4188.
- Saeyns, W., De Ketelaere, B., and Darius, P. (2008). Potential applications of functional data analysis in chemometrics. *Journal of Chemometrics*, 22(5):335–344.
- Shin, H. (2009). Partial functional linear regression. *Journal of Statistical Planning and Inference*, 139(10):3405–3418.
- Sørensen, L. K., Lund, M., and Juul, B. (2003). Accuracy of fourier transform infrared spectrometry in determination of casein in dairy cows’ milk. *Journal of Dairy Research*, 70(4):445–452.
- Soyeurt, H., Dardenne, P., Dehareng, F., Lognay, G., Veselko, D., Marlier, M., Bertozzi, C., Mayeres, P., and Gengler, N. (2006). Estimating fatty acid content in cow milk using mid-infrared spectrometry. *Journal of Dairy Science*, 89(9):3690–3695.
- Talari, A. C. S., Martinez, M. A. G., Movasaghi, Z., Rehman, S., and Rehman, I. U. (2017). Advances in fourier transform infrared (ftir) spectroscopy of biological tissues. *Applied Spectroscopy Reviews*, 52(5):456–506.
- Tennyson, J. (2019). *Astronomical Spectroscopy: An Introduction to the Atomic and Molecular Physics of Astronomical Spectroscopy*. World Scientific.
- Tibshirani, R., Saunders, M., Rosset, S., Zhu, J., and Knight, K. (2005). Sparsity and smoothness via the fused lasso. *Journal of the Royal Statistical Society: Series B (Statistical Methodology)*, 67(1):91–108.

- Tibshirani, R. J. (2014). Adaptive piecewise polynomial estimation via trend filtering. *The Annals of Statistics*, 42(1):285 – 323.
- Tibshirani, R. J. and Taylor, J. (2011). The solution path of the generalized lasso. *The Annals of Statistics*, 39(3):1335 – 1371.
- Van Der Ven, C., Muresan, S., Gruppen, H., De Bont, D. B., Merck, K. B., and Voragen, A. G. (2002). Ftir spectra of whey and casein hydrolysates in relation to their functional properties. *Journal of Agricultural and Food Chemistry*, 50(24):6943–6950.
- Visentin, G., McDermott, A., McParland, S., Berry, D. P., Kenny, O., Brodkorb, A., Fenelon, M. A., and De Marchi, M. (2015). Prediction of bovine milk technological traits from mid-infrared spectroscopy analysis in dairy cows. *Journal of Dairy Science*, 98(9):6620–6629.
- Visentin, G., Penasa, M., Gottardo, P., Cassandro, M., and De Marchi, M. (2016). Predictive ability of mid-infrared spectroscopy for major mineral composition and coagulation traits of bovine milk by using the uninformative variable selection algorithm. *Journal of Dairy Science*, 99(10):8137–8145.
- Visser, S., Slangen, C. J., and Rollema, H. S. (1991). Phenotyping of bovine milk proteins by reversed-phase high-performance liquid chromatography. *Journal of Chromatography A*, 548:361–370.
- Wahba, G. (1990). *Spline Models for Observational Data*. Society for Industrial and Applied Mathematics.
- Wedholm, A., Larsen, L., Lindmark-Månsson, H., Karlsson, A., and Andrén, A. (2006). Effect of protein composition on the cheese-making properties of milk from individual dairy cows. *Journal of Dairy Science*, 89(9):3296–3305.
- Yang, J., Zhu, H., Choi, T., and Cox, D. D. (2016). Smoothing and mean–covariance estimation of functional data with a bayesian hierarchical model. *Bayesian Analysis*, 11(3):649.
- Yao, F., Müller, H.-G., and Wang, J.-L. (2005). Functional linear regression analysis for longitudinal data. *The Annals of Statistics*, 33(6):2873 – 2903.
- Zhao, Y., Ogden, R. T., and Reiss, P. T. (2012). Wavelet-based lasso in functional linear regression. *Journal of Computational and Graphical Statistics*, 21(3):600–617.
- Zhou, S. and Shen, X. (2001). Spatially adaptive regression splines and accurate knot selection schemes. *Journal of the American Statistical Association*, 96(453):247–259.